

## ICRF HEATING AND TRANSPORT OF DEUTERIUM-TRITIUM PLASMAS IN TFTR

M. Murakami, D. B. Batchelor, C. E. Bush, A. C. England, R. C. Goldfinger, G. R. Hanson, E. F. Jaeger, D. A. Rasmussen, C. Y. Wang<sup>†</sup>, J. B. Wilgen  
Oak Ridge National Laboratory  
P. O. Box 2009  
Oak Ridge, Tennessee 37831-8072 USA

M. G. Bell, R. V. Budny, N. L. Bretz, D. Darrow, E. Fredrickson, G. Hammett, J. C. Hosea, R. Majeski, H. K. Park, C. K. Phillips, J. H. Rogers, G. Schilling, S. D. Scott, J. E. Stevens, E. Synakowski, G. Taylor, R. M. Wieland, J. R. Wilson  
Princeton Plasma Physics Laboratory  
P. O. Box 451  
Princeton, New Jersey 08543 USA

### ABSTRACT

This paper describes results of the first experiments utilizing high-power ion cyclotron range of frequency (ICRF) to heat deuterium-tritium (D-T) plasmas in reactor-relevant regimes on the Tokamak Fusion Test Reactor (TFTR). Results from these experiments have demonstrated efficient core, second harmonic, tritium heating of D-T supershot plasmas with tritium concentrations ranging from 6%-40%. Significant direct ion heating on the order of 60% of the input radio frequency (rf) power has been observed. The measured deposition profiles are in good agreement with two-dimensional modeling code predictions. Confinement in an rf-heated supershot is at least similar to that without rf, and possibly better in the electron channel. Efficient electron heating via mode conversion of fast waves to ion Bernstein waves (IBW) has been demonstrated in ohmic, deuterium-deuterium and DT-neutral beam injection plasmas with high concentrations of minority  $^3\text{He}$  ( $n_{^3\text{He}}/n_e > 10\%$ ). By changing the  $^3\text{He}$  concentration or the toroidal field strength, the location of the mode-conversion radius was varied. The power deposition profile measured with rf power modulation showed that up to 70% of the power can be deposited on electrons at an off-axis position. Preliminary results with up to 4 MW coupled into the plasma by 90-degree phased antennas showed directional propagation of the mode-converted IBW. Heat wave propagation showed no strong inward thermal pinch in off-axis heating of an ohmically-heated (OH) target plasma in TFTR.

### I. INTRODUCTION

Future fusion devices, such as the International Thermonuclear Experimental Reactor (ITER), emphasize ion cyclotron range of frequency (ICRF) heating and current drive (CD). Wave coupling at the second harmonic of the tritium cyclotron resonance ( $2\Omega_T$ ) is the proposed heating scenario in ITER deuterium-tritium (D-T) opera-

tion, but until now, no experimental data have been available. The Tokamak Fusion Test Reactor (TFTR) has performed the first experiments on ICRF heating of D-T plasmas showing significant ion heating in the  $2\Omega_T$  regime.<sup>[1,2]</sup> An increasing emphasis is being placed on control of the plasma current profile in order to access the Advanced Tokamak operating regime in future devices, such as the Tokamak Physics Experiment (TPX). Mode conversion to ion Bernstein waves (IBW) has been proposed for profile control, and, in particular, off-axis heating and CD.<sup>[3]</sup> Efficient mode conversion electron heating has been demonstrated for the first time in TFTR in  $^3\text{He}$ - $^4\text{He}$  plasmas.<sup>[4]</sup> Benchmarking this experimental data with the rf computer codes, which are needed for designing future devices, has been facilitated by rf power modulation.

This paper reviews the recent TFTR ICRF experiments. Section II describes ICRF heating in D-T plasmas, demonstrating second harmonic tritium heating, the benchmarking of rf modeling, and comparison of confinement of rf-heated D-T supershots with those heated by neutral beam injection (NBI) alone. Section III describes experiments on mode conversion of fast waves to IBWs, demonstrating efficient mode conversion (on- and off-axis), and testing for an inward thermal pinch by the use of off-axis heating. Section IV describes future plans.

### II. ICRF HEATING IN D-T PLASMAS

The initial series of experiments had two main experimental objectives: to investigate the physics of ICRF-heated plasmas in the  $2\Omega_T$  regime and to enhance the performance of D-T supershots. Plasma reactivity can be increased by directly heating tritium ions via second harmonic ICRF. Significant increases in the central electron heating of supershots via direct electron heating or collisional heating with minority tail ions may result in the lengthening of the alpha particle slowing time and an enhancement of the alpha particle pressure in D-T plasmas, facilitating investigation of alpha-particle effects in TFTR. Transport in these rf-heated D-T discharges is of significant interest.

<sup>†</sup> Oak Ridge Associated Universities

## **DISCLAIMER**

**Portions of this document may be illegible in electronic image products. Images are produced from the best available original document.**

A total of 21 D-T supershot target plasmas driven by 18 to 24 MW of  $\approx 100$ -keV NBI were heated with ICRF power launched by up to four antennas located at the midplane on the low-field side of the torus.<sup>[5]</sup> Input power of up to 5.8 MW was coupled to D-T full-size (major radius,  $R_0$ , of 2.62 m, and minor radius,  $a$ , of 0.96 m) plasmas at an rf frequency of 43 MHz with out-of-phase current strap excitation. To elucidate heating mechanisms, two systematic scans were conducted: (1) a tritium concentration scan with  $\eta_T (\equiv n_T/n_e)$  ranging from 6%–40% by varying the ratio of injected tritium to deuterium neutral beams, and (2) a toroidal field scan to vary the location of the  $2\Omega_T$  layer relative to the magnetic axis.

RF power modulation provides a technique for directly measuring the ICRF power absorption characteristics by examining the time response of the measured ion- and electron-stored energies to the rf power modulation.<sup>[6]</sup> The electron-stored energy was computed from the electron temperature response, which was measured by electron cyclotron emission (ECE) and combined with the electron density profile, obtained by a multi-channel far infrared interferometer (MIRI). The ion stored energy was computed from the charge exchange spectroscopy (CHERS) measurement of  $T_i$  combined with the thermal ion density calculated by the TRANSP code which was in turn based on the electron density,  $Z_{eff}$  (obtained from visible bremsstrahlung) and a Monte Carlo beam deposition model. The electron and ion heating power per unit volume can be inferred from: (1) the change in the time-derivative of the electron and ion energy density when the rf power was turned on or off, and (2) the Fourier transform carried out over several cycles of modulation.

Figure 1 shows the local ion and electron power deposition profiles (for a 1-MW power input to the

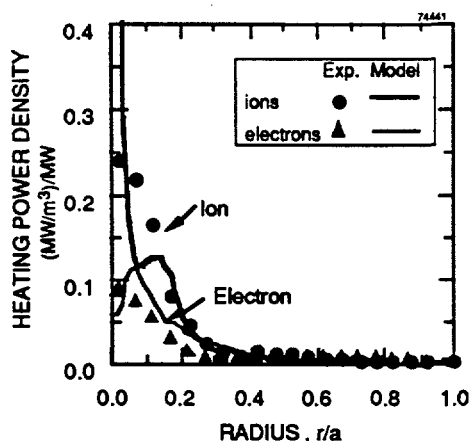


Fig. 1. Ion and electron heating power density as a function of radius measured (solid circles and triangles) with the modulation technique. The continuous curves are the heating power density profiles predicted by the PICES code. Data are given for D-T supershot plasmas with 3.6 to 3.7 MW of ICRF power, 17 to 20 MW of NBI power, with the  $2\Omega_T$  resonance layer on axis, and with residual concentrations of  $^3\text{He}$  estimated at 0.2%.

antenna) obtained from the modulation analysis for a plasma in which the  $2\Omega_T$  layer was located at the magnetic axis and with 60% tritium in NBI [ $B_T = 4.6$  T,  $P_{bT}/(P_{bD}+P_{bT}) = 0.6$ ]. The central portion of the ion and electron local power deposition can be expressed as Gaussians,  $\exp[(\rho/\alpha)^2]$ , with  $\alpha = 0.17$  and  $0.16$ , respectively, where  $\rho$  is the normalized minor radius  $r/a$ . The volume integrated values of the curves give the power absorption (within  $r = a$  with uncertainties in the analysis) of  $59 \pm 10\%$  for ions and  $26 \pm 3\%$  for electrons. The total absorption,  $85 \pm 10\%$ , is consistent with the value,  $80 \pm 10\%$ , estimated by magnetic analysis.

The rf modeling predictions are compared favorably with the experimental results determined by rf modulation. The curves overlaying the experimental points in Figure 1 are the ion and electron heating power deposition profiles predicted by the PICES code.<sup>[7]</sup> PICES is a two-dimensional (2-D), reduced-order, full wave code, with multiple (80) toroidal mode numbers for representation of the launched antenna spectrum and is based on the experimental temperature and density profiles (including beam ions with an effective temperature of  $\sim 60$  keV on axis). The calculated radial power density profiles are similar to the experimental measurements. Of the total rf power, 26% of the rf power was absorbed directly by electrons via Landau damping and transit time magnetic pumping near the core, in good agreement with rf modulation data. Of the 49% ion absorption, 43% was absorbed at the  $2\Omega_T$  resonance near the core and 6% at the D (and carbon) fundamental resonance located at  $r/a = 0.7$ . This code also predicts that  $\sim 16\%$  of the rf power was absorbed at the intersection of deuterium ion fundamental resonance ( $R \approx 2.1$  m) and the mode conversion layer near the last closed flux surface. There is so far no experimental evidence to support (or refute) this effect. Power deposition profiles were also obtained for the same plasma with the rf package in TRANSP, consisting of a 2-D reduced-order wave solver, SPRUCE,<sup>[8]</sup> combined with the bounce-averaged Fokker-Planck solver, FPP.<sup>[9]</sup> From this analysis, 24% of the power was absorbed by electrons and 63% by ions within  $r/a = 0.85$ . The differences between the results of PICES and TRANSP appear to stem from the difference in the multiple and single mode calculations. The power splits predicted by both codes are in relatively close agreement with the data.

There is also good agreement between the experimental power splits and the model predictions in the tritium concentration scan with the  $2\Omega_T$  layer on axis. The observed trends in the data (see Figure 2) are consistent with the theoretical prediction that the  $2\Omega_T$  heating efficiency increases with the tritium beta. Up to  $59 \pm 10\%$  of the rf power was observed to be absorbed by ions. The core  $2\Omega_T$  heating is strong even for  $\eta_T$  as low as  $\sim 6\%$  (15% of NBI power in T) primarily due to the presence of hot tritium beam ions. Further experimental

evidence exists in support of core  $2\Omega_T$  absorption: (1) a  $B_T$  scan showed that the ion heating peaks at the  $2\Omega_T$

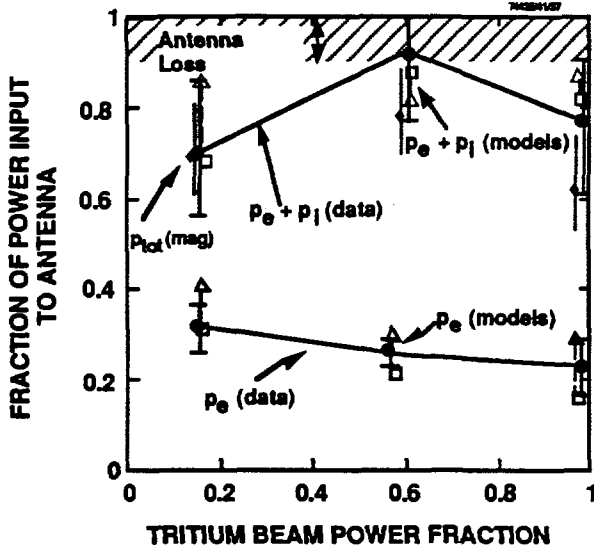


Fig. 2. Dependence of the fraction of power absorbed directly by electrons and ions is shown as a function of tritium beam power fraction during rf modulation. Data are given for D-T supershot plasmas with 3.6 to 3.7 MW of ICRF power, 17 to 20 MW of NBI power, with the  $2\Omega_T$  resonance layer on axis, and with residual concentrations of  $^3\text{He}$  estimated at 0.2%.

layer on axis, which is in agreement with the models<sup>[2]</sup>; and (2) the fast ion loss detectors observed escaping tritium tail ions (of  $\sim 600$  keV) synchronously with rf modulation.<sup>[10]</sup>

The addition of 5.8 MW of ICRF power to a D-T supershot resulted in a significant increase in the core ion and electron temperatures<sup>[1]</sup>, as shown in Figures 3a and 3b. A plasma line average density of about  $4 \times 10^{19} \text{ m}^{-3}$  was established by NBI, and 2%  $^3\text{He}$  gas was added to minimize effects of rf eigenmode excitation. The 43-MHz ICRF waves were resonant with both the minority  $^3\text{He}$  ( $\omega \sim \Omega_{^3\text{He}}$ ) and the majority tritium ( $\omega \sim 2\Omega_T$ ) near the Shafranov-shifted magnetic axis ( $B_T = 4.2$  T at  $R = 2.83$  m). The central ion temperature, measured by CHERS, increased from 26 to 36 keV. The central electron temperature, as measured by ECE, increased from 8 to 10.5 keV, due to a combination of direct electron heating via Landau damping and collisions with minority tail ions. There was also a 10% increase in the D-T neutron production rate to  $\sim 1.2 \times 10^{18} \text{ s}^{-1}$  during the early part of the discharge; however, the performance was spoiled by an enhanced carbon influx that began at about 3.4 s due to plasma moving to an unconditioned portion of the limiter. Figures 3c and 3d show the measured ICRF heating power density added to the NBI power density for ions and electrons. The additions are significant out to  $r/a \sim 0.3$ , leading to the increase in  $T_i$  and  $T_e$  there. The observed core ion heating is consistent

with  $2\Omega_T$  heating, because an analogous increase was not evident in the earlier D ( $^3\text{He}$ ) experiments.<sup>[11]</sup> Furthermore, a core ion temperature of 32 keV was obtained with only 4.4 MW of ICRF power during a companion discharge that was essentially identical to the present case without  $^3\text{He}$  added.

Measurements of the electron and ion heating power density allow the examination of the effects of transport in rf-heated plasmas relative to that with NBI alone. To avoid prescribing a particular convective multiplier (3/2 or 5/2), the local transport is characterized by the total effective diffusivity  $\chi^{\text{tot}}\{i,e\}$ , which is the ratio of the total radial ion and electron heat flux to the corresponding temperature gradient. The same conclusions can be drawn from the usual ion and electron thermal diffusivity analysis. Figures 3e and 3f show the total effective heat diffusivity for ions and electrons as a function of radius with the measured rf power deposition profiles incorporated in the post-TRANSP analysis. There is no significant difference between the  $\chi^{\text{tot}}\{i\}$  profile with and without rf, indicating that  $T_i(r)$  increases with rf power while roughly maintaining  $\chi_i$ . Electron transport is even more favorable with rf. It showed a reduction in  $\chi^{\text{tot}}\{e\}$  by almost factor of 2 in the radii outside  $\rho = 0.4$ . So confinement of rf-heated D-T plasmas is at least similar to that with NBI alone, and possibly better in the electron channel. Inclusion of rf-driven ripple loss may indicate more favorable ion transport for rf-heated shots.<sup>[12]</sup>

### III. MODE CONVERSION EXPERIMENTS

Recently, a novel technique for localized electron heating and CD utilizing efficient mode conversion of fast magneto sonic waves into IBW at ion-ion hybrid layers has been suggested by Majeski et al.<sup>[3]</sup> This technique is D-T compatible, uses no extra hardware, and may provide off-axis CD to access the advanced tokamak operating regime. In contrast to mode conversion in the conventional minority heating scheme utilizing a small minority ion concentration, the proposed scheme enhances the mode conversion efficiency (and thereby the electron heating efficiency) by: (1) separating the mode conversion layer (at the two-ion hybrid layer  $n_{//}^2 = S$ ) from the cyclotron layer; and (2) forming a closely spaced "cutoff-resonance-cutoff" triplet.

Experiments performed on TFTR in D- $^4\text{He}$  plasmas with a high  $^3\text{He}$  concentration ( $n_{^3\text{He}}/n_e \approx 25\%$ ) have demonstrated efficient mode conversion electron heating on and off axis. With the mode conversion layer located on axis and far away from the cyclotron resonance ( $\Omega_{^3\text{He}}$  at  $\rho = 0.3$  on the low-field side), highly peaked electron temperature profiles with central temperatures reaching the 8 to 10 keV range (as measured by Thomson scattering and ECE diagnostics) heated by only 2 to 3 MW of incident rf power have been observed. The

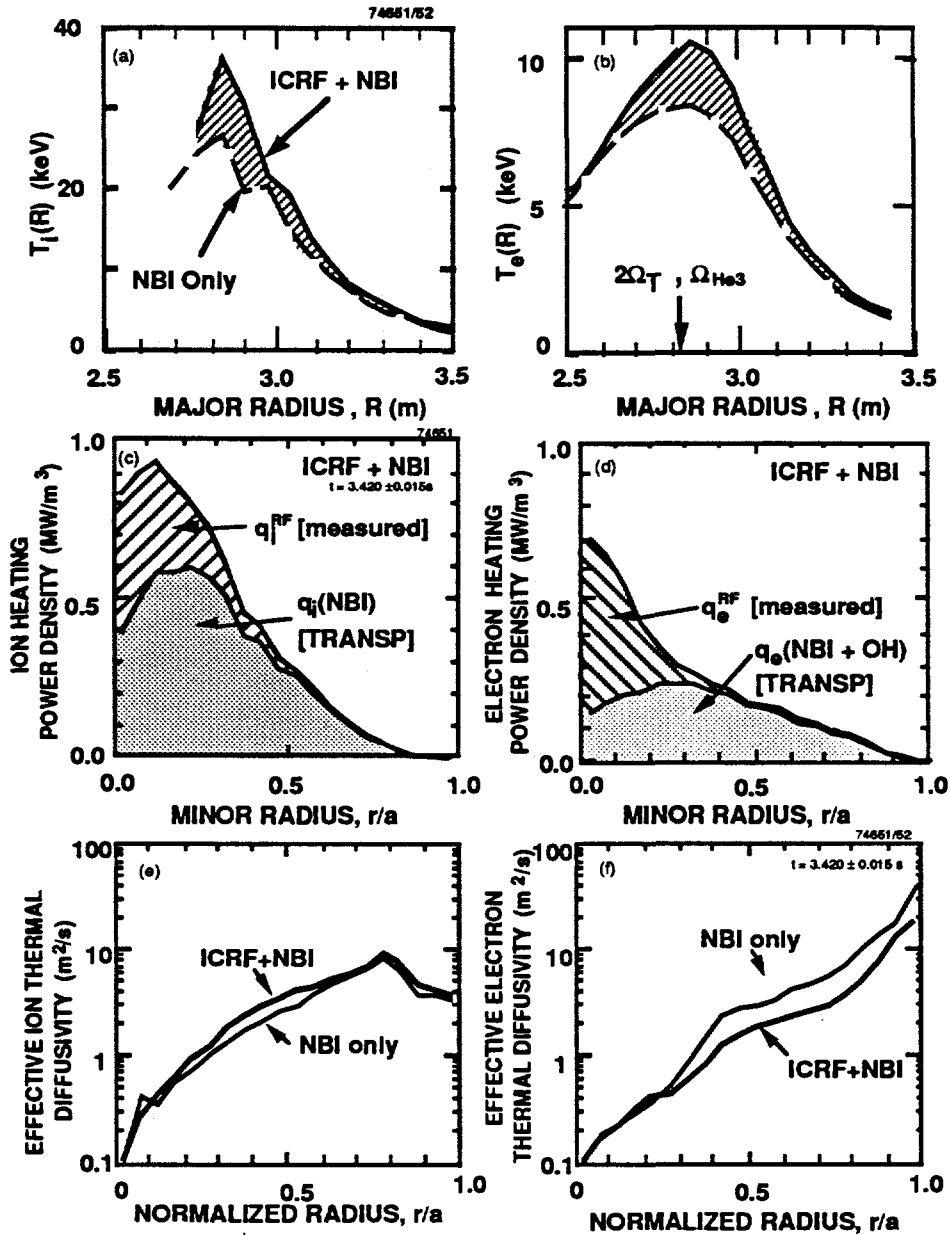


Fig. 3. Comparison of (a) ion and (b) electron temperature profiles, (c) ion and (d) electron heating power density profiles, and (e) ion and (f) electron total effective thermal diffusivity profiles for two plasmas with 23.5 MW of neutral beam injection (60% in tritium). The plasma indicated by the solid line had 5.5 MW of 43-MHz ICRF heating resonant with the  $2\Omega_T$  cyclotron layer on the magnetic axis at  $R = 2.82$  m. Both plasmas had a 2%  $^3\text{He}$  minority, the fundamental resonance of which is degenerate with the  $2\Omega_T$  resonance.

fraction of the power mode converted and coupled to electrons rises with the  $^3\text{He}$  concentration, from 0.2 at  $n_{^3\text{He}}/n_e < 10\%$  (close to the conventional minority heating regime) to  $>50\%$  typical (as high as 80%) for  $n_{^3\text{He}}/n_e = 15\%$  to 30%. Figure 4 shows the measured major radius of the peak of the electron power deposition profile as a function of the toroidal field for a constant density [ $n_e(0) = 4 \times 10^{19} \text{ m}^{-3}$ ] and  $^3\text{He}$  fraction (0.14). The power deposition radius occurs within a few centimeters of the two-ion hybrid layer ( $n_{||}^2 = S$ ) which is

away from the cyclotron resonance ( $\Omega_{^3\text{He}}$ ) and whose distance from the magnetic axis increases with decreasing magnetic field.

Figure 5 shows the rf heating profile measured by the modulation technique for a discharge in which the mode conversion surface was located at  $r/a \approx 0.2$  on the high-field side of the magnetic axis. This plasma had a central electron density of  $\sim 4 \times 10^{19} \text{ m}^{-3}$ , a central electron temperature of 5 keV, and profiles that were approximately parabolic. CHERS measurements from similar discharges imply a central ion temperature of about 4 keV

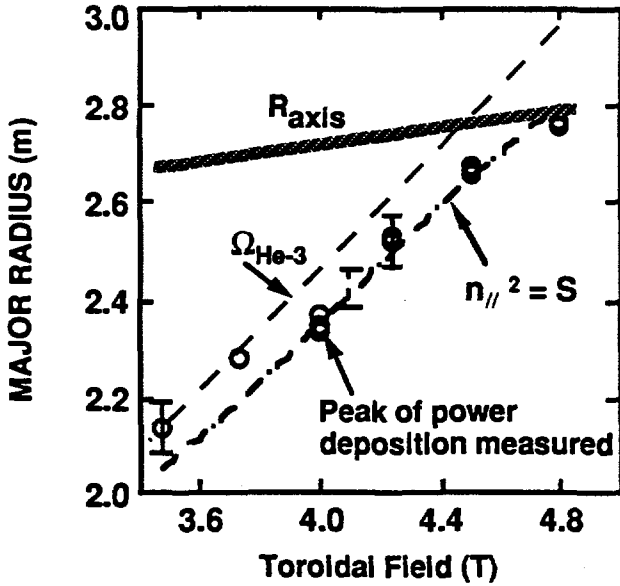


Fig. 4. Dependence of the major radius (open circles) of the peak of electron absorbed power determined by power modulation techniques as a function of toroidal magnetic field intensity for constant  ${}^3\text{He}$  fraction ( $n_{{}^3\text{He}}/n_e = 0.14$ ) and constant density ( $n_e(0) = 4 \times 10^{19} \text{ m}^{-3}$ ). The chained line denotes the calculated position of the mode conversion layer, the dashed line denotes the  ${}^3\text{He}$  cyclotron layer, and the shaded thick line denotes the approximate typical position of the magnetic axis in the discharges shown.

for this plasma. The measured power absorption by electrons is contrasted with model calculations in Figure 5. The analyses obtained with the 1-D kinetic wave codes, FELICE<sup>[13]</sup> and GLOSI<sup>[14]</sup>, show good agreement with the observed deposition radius, although the predicted profiles are narrower than the experimental

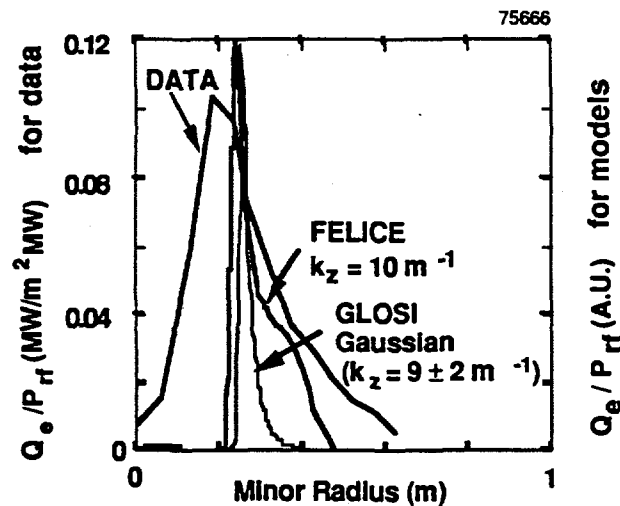


Fig. 5. The ICRF power deposition profile of the electrons, derived from power modulation techniques, is contrasted with model predictions of 1-D codes (FELICE and GLOSI) for off-axis mode conversion on the high field side of the magnetic axis.

profiles, probably due to wave focusing and neglect of poloidal variations in the equilibrium. The measured net power coupled to the electrons is observed to be about 70% of the total rf input power, with only a small amount, ~5%, deposited near the magnetic axis via direct electron Landau damping. While the FELICE code result is based on a single  $k_{||}$  ( $=10 \text{ m}^{-1}$ ), the GLOSI code result is based on an average of multiple  $k_{||}$  calculations with a power weighting function of a Gaussian form,  $\exp[-((k_{||} - 9)/2)^2]$  to average out the standing wave pattern in the rf field within the triplet.<sup>[3]</sup> The electron absorption predicted by both codes is 82%.

With directional excitation of the incident fast waves, damping of mode-converted IBW should lead to localized rf-induced CD. Unlike standard fast wave CD that relies on direct electron Landau damping in the core, this technique can provide localized CD at a minor radius that can be controlled by varying the location of the  $n_{||}^2 = S$  layer. Initial tests of this concept were performed in D- ${}^4\text{He}$ - ${}^3\text{He}$  plasmas with 2.2 MW of ICRF power launched with  $\pm 90^\circ$  antenna phasing to provide a directional fast wave with  $k_{||} \sim 6 \text{ m}^{-1}$  at the antenna. The mode conversion layer was placed near the magnetic axis for the rf frequency of 43 MHz,  $B_T = 4.5 \text{ T}$ ,  $\eta_{{}^3\text{He}} \sim 12\%$ , and  $n_e(0) = 4 \times 10^{19} \text{ m}^{-3}$ . Though the observed electron temperature response was distinctly different for  $+90^\circ$  and  $-90^\circ$  launch, the measured surface voltage was essentially the same for these two cases in spite of expectation of rf-driven currents in the range of 100 to 200 kA. Subsequent TRANSP modeling indicated that centrally rf-driven currents of this magnitude are insufficient to modify the surface voltage on the time scale of the rf pulse (0.8 s). Nevertheless, these results indicate that the mode converted IBW is directional. Future CD experiments will be performed with longer rf pulses and more direct measurements of the current profile by the motional Stark effect.

Off-axis mode conversion electron heating was used to study the inward thermal pinch, which is a transport phenomena that is currently under discussion for toroidal plasmas. A strong inward thermal pinch was observed with off-axis electron cyclotron heated (ECH)-plasmas in DIII-D.<sup>[15]</sup> Because no strong inward pinch was observed in Wendelstein VII-Advanced Stellarator (WVII-AS) ECH off-axis experiments<sup>[16]</sup>, the question may be asked whether this is specific to tokamaks.

During the Toki conference, Dr. Kadomtsev<sup>[17]</sup> offered an explanation for the phenomena via a trapped particle effect of ECH electrons with primarily perpendicular energy. Since the present heating tends to increase the parallel energy component, it is interesting to see how transport behavior with this heating contrasts with that of ECH. Analysis of the electron temperature response at turn-off showed sharp off-axis heating at  $\rho = 0.24$  with  $\Delta\rho$ (FWHM) of 0.17 at  $B_T = 4.2 \text{ T}$ . Radial

variations of the Fourier-transformed electron temperature ( $T_e$ ) response (Figure 6) shows that heat pulses propagate simultaneously inward and outward with similar velocities ( $d\phi/dr$ ). Furthermore, the thermal diffusivity estimated from the slope of the  $T_e$  amplitude (on a semi-logarithmic scale) and that from the phase are nearly equal, implying no substantial (inward) thermal pinch.<sup>[18]</sup> These studies will be extended to rf powers substantially larger than the ohmic power in the future.

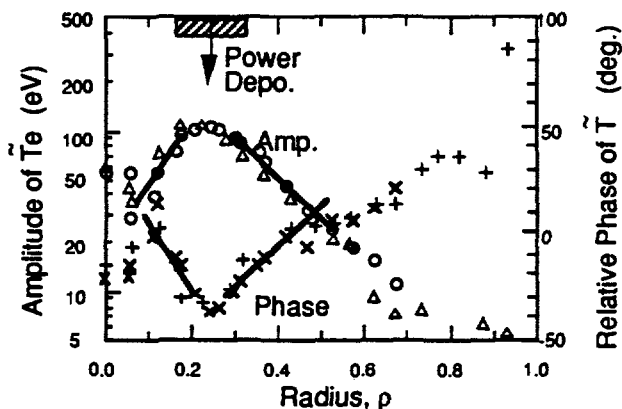


Fig. 6. Dependence of the heat pulse phase (linear scale) and amplitude (semi-logarithmic scale) vs. normalized minor radius for off-axis power deposition with mode conversion electron heating.

#### IV. CONCLUSIONS

The first experiments utilizing high-power ICRF to heat D-T plasmas in reactor-relevant regimes have been completed on TFTR. Results from these experiments have demonstrated efficient core, second harmonic tritium heating in D-T supershot plasmas with tritium concentrations ranging from 6%-40%. Significant direct ion heating on the order of 60% of the input rf power has been observed. The measured deposition profiles are in good agreement with 2-D modeling code analyses of these discharges. Based on these observations and models, efficient core  $2\Omega_T$  ICRF heating is anticipated in the higher density plasmas projected for ITER. Confinement in an rf-heated supershot is at least similar to that without rf, and possibly better in the electron channel.

Efficient, localized electron heating via mode conversion of incident fast waves to IBWs at the ion-ion hybrid layer has been documented in D- and D-T-<sup>4</sup>He plasmas with a relatively large concentration of minority <sup>3</sup>He ions. By varying the relative concentration of the ion species as well as the toroidal magnetic field for a fixed rf frequency of 43 MHz, the location of the hybrid layer was scanned between the magnetic axis out to about 40% of the minor radius on the high-field side of the discharge. The rf power modulation studies indicate that 50% or

more of the input ICRF power was damped on electrons near the mode conversion layer, consistent with theoretical predictions. The direction of propagation of the mode converted IBW was shown to depend on the propagation of the launched waves, as controlled by the antenna phasing. Heat wave propagation with off-axis heating shows no strong inward pinch in ohmically-heated target plasmas in TFTR.

Future TFTR experiments utilizing ICRF heating will focus on both supershot and L-mode regimes (ITER relevant) and increasing the pressure in D-T supershots. We will also explore  $\Omega_D$  and mode conversion heating at higher  $B_T$  and continue to develop current profile control via mode conversion CD.

#### ACKNOWLEDGMENTS

We wish to acknowledge Dr. T. C. Luce of General Atomics, and the ICRF group and TFTR project engineering and technical staff for their contribution to this work. We are grateful to Drs. R. Davidson, R. Hawryluk, H. Furth, K. McGuire, D. Meade, and P. Rutherford for their continued support. This research was sponsored by the Office of Fusion Energy, U.S. Department of Energy, under contract DE-AC05-84OR21400 with Martin Marietta Energy Systems, Inc., and DE-AC02-76-CHO-3073.

#### REFERENCES

1. G. Taylor, M. Murakami, H. Adler *et al.*, "ICRF Heating of Deuterium-Tritium Plasmas in TFTR," to be published in Proc. of Fifteenth Int. Conf. on Plasma Phys. and Controlled Nucl. Fusion Res., Seville, September 26-October 1, 1994.
2. C. K. Phillips, M. G. Bell, R. Bell, N. Bretz *et al.*, "Ion Cyclotron Range of Frequencies Heating and Current Drive in Deuterium-Tritium Plasmas," to be published in Phys. Fluids (1994).
3. R. Majeski, C. K. Phillips, and J. R. Wilson, "Electron Heating and Current Drive by Mode Converted Slow Wave," *Phys. Rev. Lett.* 73, 2204 (1994).
4. R. Majeski, N. L. Fisch, H. Adler, S. Batha *et al.*, "Mode Conversion Studies in TFTR," to be published in Proc. of Fifteenth Int. Conf. on Plasma Phys. and Controlled Nucl. Fusion Res., Seville, September 26-October 1, 1994.
5. G. Schilling *et al.*, *Proc. 10th Topical Conf. on RF Power in Plasmas*, Boston, AIP Conf. 289, 3 (1993); J. R. Wilson *et al.*, to appear in the Proc. of the 18th Symp. on Fusion Tech., Karlsruhe, Germany (1994).
6. M. Murakami, E. Fredrickson, E. F. Jaeger, D. A. Rasmussen *et al.*, "ICRF Direct Electron Heating Experiments in TFTR," *Proc. 20th European Conf. on Controlled Fusion and Plasma Phys.*, Lisbon, Portugal (EPS), vol. 3, (1993) 981.

7. E. F. Jaeger *et al.*, Nucl. Fusion 33, (1993) 179.
8. D. N. Smithe *et al.*, Nucl. Fusion 27, (1987) 1319.
9. G. W. Hammett, Ph.D. Thesis, Princeton University (1986).
10. D. S. Darrow, S. J. Zweben, R. V. Budny *et al.*, PPPL-2975 (Oct. 1994), submitted to Nucl. Fusion.
11. G. Taylor, J. R. Wilson, R. C. Goldfinger, J. C. Hosea *et al.*, Plasma Phys. Control. Fusion 34, 523 (1994).
12. M. H. Redi *et al.*, PPPL-3011, 1994.
13. M. Brambilla and T. Krücken, Nucl. Fusion 28, 1813 (1988).
14. C. Y. Wang *et al.*, to be published as an ORNL Report (1995).
15. T. C. Luce, C. C. Petty, and J. C. de Haas, "Inward Energy Transport in Tokamak Plasmas," Phys. Rev. Lett. 68, 52 (1992).
16. F. Wagner and U. Stroth, Plasma Phys. Control. Fusion (1994).
17. B. Kadomtsev, this conference.
18. T. C. Luce, C. B. Forest, M. A. Makowski, W. H. Mayer *et al.*, "Evidence from Modulated ECH for Convective-like Transport," in Proc. ISPP-14, Piero Caldirola, on Local Transport Studies in Fusion Plasmas [J. D. Callen, G. Gorini and E. Siodoni (eds.)], SIF, Bologna (1993).



## FIGURE CAPTIONS

- Fig. 1. Ion and electron heating power density as a function of radius measured (solid circles and triangles) with the modulation technique. The continuous curves are the heating power density profiles predicted by the PICES code. Data are given for D-T supershot plasmas with 3.6 to 3.7 MW of ICRF power, 17 to 20 MW of NBI power, with the  $2\Omega_T$  resonance layer on axis, and with residual concentrations of  $^3\text{He}$  estimated at 0.2%.
- Fig. 2. Dependence of the fraction of power absorbed directly by electrons and ions is shown as a function of tritium beam power fraction during rf modulation. Data are given for D-T supershot plasmas with 3.6 to 3.7 MW of ICRF power, 17 to 20 MW of NBI power, with the  $2\Omega_T$  resonance layer on axis, and with residual concentrations of  $^3\text{He}$  estimated at 0.2%.
- Fig. 3. Comparison of (a) ion and (b) electron temperature profiles, (c) ion and (d) electron heating power density profiles, and (e) ion and (f) electron total effective thermal diffusivity profiles for two plasmas with 23.5 MW of neutral beam injection (60% in tritium). The plasma indicated by the solid line had 5.5 MW of 43-MHz ICRF heating resonant with the  $2\Omega_T$  cyclotron layer on the magnetic axis at  $R = 2.82$  m. Both plasmas had a 2%  $^3\text{He}$  minority, the fundamental resonance of which is degenerate with the  $2\Omega_T$  resonance.
- Fig. 4. Dependence of the major radius (open circles) of the peak of electron absorbed power determined by power modulation techniques as a function of toroidal magnetic field intensity for constant  $^3\text{He}$  fraction ( $n_{^3\text{He}}/n_e = 0.14$ ) and constant density ( $n_e(0) = 4 \times 10^{19} \text{ m}^{-3}$ ). The chained line denotes the calculated position of the mode conversion layer, the dashed line denotes the  $^3\text{He}$  cyclotron layer, and the shaded thick line denotes the approximate typical position of the magnetic axis in the discharges shown.
- Fig. 5. The ICRF power deposition profile of the to electrons, derived from power modulation techniques, is contrasted with model predictions of 1-D codes (FELICE and GLOSI) for off-axis mode conversion on the high field side of the magnetic axis.
- Fig. 6. Dependence of the heat pulse phase (linear scale) and amplitude (semi-logarithmic scale) vs. normalized minor radius for off-axis power deposition with mode conversion electron heating.

## DISCLAIMER

This report was prepared as an account of work sponsored by an agency of the United States Government. Neither the United States Government nor any agency thereof, nor any of their employees, makes any warranty, express or implied, or assumes any legal liability or responsibility for the accuracy, completeness, or usefulness of any information, apparatus, product, or process disclosed, or represents that its use would not infringe privately owned rights. Reference herein to any specific commercial product, process, or service by trade name, trademark, manufacturer, or otherwise does not necessarily constitute or imply its endorsement, recommendation, or favoring by the United States Government or any agency thereof. The views and opinions of authors expressed herein do not necessarily state or reflect those of the United States Government or any agency thereof.